Pole Arc Skewing Analysis of Synchronous Reluctance Machine Using Discrete Method Combined with Winding Function Approach

P. Naderi and A. Shiri

Electrical Engineering Department
Shahid Rajaee Teacher Training University, Tehran, 1678815811, Iran
p.naderi@srttu.edu, abbas.shiri@srttu.edu

Abstract ─ The paper investigates the effect of pole arc skewing in synchronous reluctance machine on its torque ripple. To do this, the machine's reluctances are calculated by using winding function approach (WFA). A numerical-based method is proposed for modeling the machine's dynamic equations. The effect of rotor skewing and the winding type (single-layer or double layer) on the machine's behavior and torque ripple are investigated. The results show that skewing the rotor is significantly effective in double-layer winding case and it is not a proper idea for machine with single-layer winding. The proposed method is capable of studying the voltage-fed machine's behavior which is common in reality in comparison with current source-fed machine. Also, shorter calculation time and capability of studying parameter sensitivity are other advantages of the proposed method in comparison with finite element method (FEM).

Index Terms ─ Air-gap function, rotor skewing, slot opening, winding function.

I. INTRODUCTION

The synchronous reluctance machine (SynRM) has been widely employed in industry such as high speed applications and vehicular technology. Besides having high efficiency, these motors have working ability in variable frequency conditions. In many researches, the torque produced by the SynRM is supposed smooth; however, a real machine has some torque/current ripples due to some effects including slot opening and also limited slot numbers which make the winding function and magneto-motive force (MMF) non-sinusoidal. In this paper, by using winding function approach (WFA), rotor skewing, pole arc changing and also winding chording are analyzed in order to reduce the torque ripple. The WFA is a powerful tool for electrical machine modeling which has some advantages in comparison with FEM [1]-[4]. In [1], using WFA, the pole skewing is addressed for torque ripple reduction in SynRM. The machine performance is studied in both single and double-layer winding case. Lubin, et. al., have

modeled a 4-pole SynRM using both FEM and WFA and the results have been compared [2]. In both mentioned references, the three-phase sinusoidal current source has been used as power supply which is not usual in reality. In [2], only a single-layer winding machine has been modeled by FEM and WFA, and the pole skewing is not considered in investigations. However, in [1], the pole skewing effect in double-layer winding machine has been presented. In the mentioned references, the machine performance has not been studied in voltage feed conditions. The synchronous machine has been also modeled in some researches for behavior studying and fault detection. In [3], using WFA, eccentricity fault effect has been addressed by Jocsimovich, et. al.; however, slot opening effect has not been considered in modeling. In another work, eccentricity fault have been studied by Faiz, et. al., for induction machine using WFA; however, only two simple windings have been considered and ideal air-gap function has been used [4]. In [5], WFA has been used for dynamic eccentricity fault diagnosis. In [6], the effect of slot and pole combination has been addressed for performance analysis of tooth-coil synchronous machine by winding harmonic spectrum analysis. In this reference, the slot opening effect has not been considered. In [7], by simplifying the model (which reduces the accuracy of the results) and considering some damper bars for the machine and using electromagnetic equations, fault detection has been discussed. By taking in to account suitable design modifications, such as multiple flux barriers, axially laminated anisotropic rotor instead of regular induction motor rotor, the poor power factor of the SynRM has been improved [8]-[11]. Although, ideal machines can be modeled by using classical approaches such as *dq* transformation, these kinds of modeling ignore all the space harmonics; therefore, they are not suitable for exact studying of the real machines [12]. In modeling of the real machine, the effects such as slot openings and distributed winding functions should be considered in the air-gap function. The latter is very important for eccentricity fault detection. Considering the above-mentioned facts, an advanced method should be used for

space harmonics analysis and eccentricity fault detection instead of the classical methods [13]-[16].

In this paper, a sample SynRM is modeled using WFA and inductance calculations in cases of skewed and un-skewed rotor are done. Then, to compute the currents, torque, etc., an iteration-based numerical method has been proposed for modeling of the machine's dynamical equation. The proposed method gives different results in comparison with those appeared in [1].

The results show that the skewing is an effective tool for torque ripple reduction in both single and double-layer windings; however, in single-layer winding, the reduction of torque ripple is not considerable. By applying a three phase sinusoidal current to the stator winding as done in [1], it is shown that the torque ripple is considerably reduced due to rotor skewing. Due to the fact that the motor is supplied by voltage source in reality, the latter is investigated in this paper which shows different results in comparison to [1], in which the machine has been fed by current source, especially in case of single-layer winding.

II. PROBLEM DEFINATION

Torque ripple calculation of a three-phase four-pole SynRM is considered in this research (Fig. 1) which has been studied in [1] with the same structure. Stator has 36 slots where three slots have been assigned for each pole per phase. As shown in Fig. 1, the stator reference ($\theta_s = 0$) is supposed in the center of the phase 'A' winding, while the rotor reference ($\theta_r = 0$) is set to the maximum air-gap length. Supposing the number of turns per pole per phase to be N_s, there exists the number of Ns/3 turns in each slot in single-layer winding and the number of $N_s/6$ turns in each slot in double-layer case. Clearly, the multi-layer winding reduces space harmonics produced by distributed windings; however, it has not any effect on the harmonics produced by the number of the slots and also slot openings. In [1], pole skewing has been proposed for reduction of space harmonics which is reconsidered in this paper to obtain extended results. The pole skewing is shown in Fig. 2. Calculations will be done for different scenarios to obtain extended results and the latter will be compared with the results in [1]. The machine parameters are shown in Table 1. In the following section, some phenomena involved in the dynamic modeling of the machine, are discussed.

III. MODELING OF THE SLOT OPENING AND THE POLE SALIENCY

One of the non-ideal features of a real machine is slot opening geometry. The proper function should be defined for rotor poles and slot opening for accuracy of the modeling. Geometrical structure of rotor poles and stator slots are shown in Fig. 3.

A. Rotor's poles

Referring to geometric parameters shown in Fig. 3, the rotor pole saliency for one of the inter-polar-gap can be written as [2]:

$$g_r(\varphi) = \frac{r.(\pi/2 - |2\varphi + \beta|).[\text{Sin}(|2\varphi + \beta|) - \text{Sin}(\beta)]}{\text{Cos}(2\varphi + \beta)} \quad (1)$$

for $0 \leq \varphi \leq \lambda$,

where all angles are mechanical as shown in Fig. 3 and r is the inner radius of the stator. Since the rotor has 4 poles, the gap function of these poles can be mathematically modeled as:

$$f_{r1}(\theta_r) = g_r(\theta_r).[u(\theta_r) - u(\theta_r - \pi/2 + \beta)], \quad (2)$$

$$f_r(\theta_r, x) = \sum_{k=-4}^{4} f_{r1}\left(\theta_r - \alpha_{sk}\,x/l\right. \\ \left. + (\pi - 2\beta)/4 - k\,\pi/2\right). \quad (3)$$

In the above equations, $\theta_r = \theta_s - \theta_m$ and $0 < x < l$.

Single-layer winding
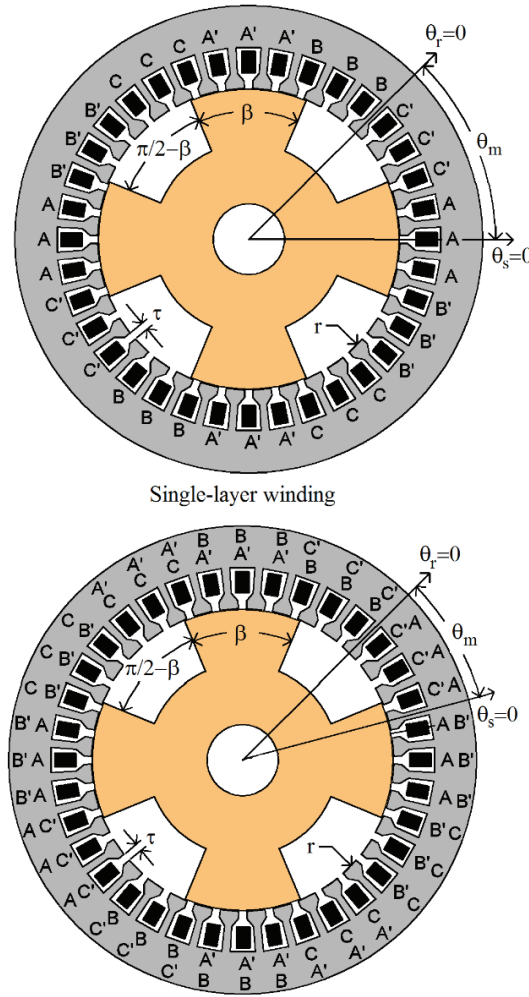
Fig. 1. The SynRM structure.
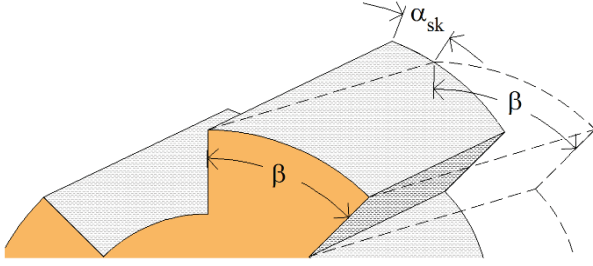
Fig. 2. Illustration of pole skewing.

Table 1: Geometrical and electrical specifications of the machine [1]

Symbol	Parameter	Value
N_s	Turns per pole	90
β	Pole saliency	45° (un-skewed)
R_s	Winding resistance	2 Ω
τ	Angle of slot opening	3°
g_o	Air-gap	0.26 mm
Yn	Windings connection	Star grounded
r	Stator radius	4.5 cm
l	Machine length	15.5 cm
l_{ls}	Leakage inductance	1 mH
b0,b1	Slot width properties	2.97, 7.51 mm
h0,h1	Slot depth properties	3.71, 3.51 mm
N_{slot}	Number of slots	36
P	Number of poles	4
γ	Slot pitch	$10°$
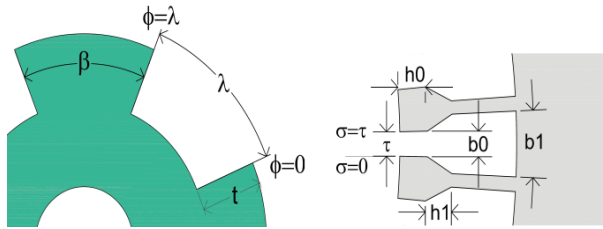
Fig. 3. Geometrical structure of rotor poles and stator slots.

B. Slot opening modeling

The slot opening for a half-gap can be written as follows [2]:

$$g_s(\sigma)=
\begin{cases}
\pi/2 . r . \sigma & 0 \leq r.\sigma \leq h0 \\
\pi/2 . r . \sigma + \varepsilon(r.\sigma - h0) & h0 \leq r.\sigma \leq \frac{\tau}{2}
\end{cases}, \quad (4)$$
$$\text{for } 0 \leq \sigma \leq \tau/2$$

$$\varepsilon = \pi/2 - \text{Tan}^{-1}(2h1/(b1 - b0)). \quad (5)$$

The gap function for slot openings can be modeled as:

$$f_{s1}(\theta_s) = g_s(\theta_s).[u(\theta_s) - u(\theta_s - \tau/2)], \quad (6)$$

$$f_{s2}(\theta_s) = f_{s1}(\theta_s) + f_{s1}(-\theta_s + \tau). \quad (7)$$

Using the above equations and considering that the stator has 36 slots, we can wright:

For single-layer winding:

$$f_s(\theta_s) = \sum_{k=0}^{36} f_{s2}(\theta_s + \tau/2 - k\,(2\pi/36)), \quad \text{(8-a)}$$

For double-layer winding:

$$f_s(\theta_s) = \sum_{k=0}^{36} f_{s2}(\theta_s + \tau/2 + \pi/N_{slot} \\ - k\,(2\pi/36)). \quad \text{(8-b)}$$

C. Total air gap function

The total air-gap function consists of three parts including slot openings, rotor saliency and conventional air-gap which can be written as follows:

$$f_g(\theta_s, \theta_m, x) = f_s(\theta_s) + f_r(\theta_s, \theta_m, x) + g_0, \quad (9)$$

where g_0 is the constant air-gap between the stator teeth and rotor saliency and also $\theta_r = \theta_s - \theta_m$. So, as it is seen in (2)-(9), the air-gap is a function of pole skewing (α_{sk}), mechanical rotor position (θ_m), and also mechanical angle of stator (θ_s). The air-gap function for stator slot and rotor saliency is plotted in Fig. 4 for a sample case with 22.5 degrees skewing.

(a)

(b)
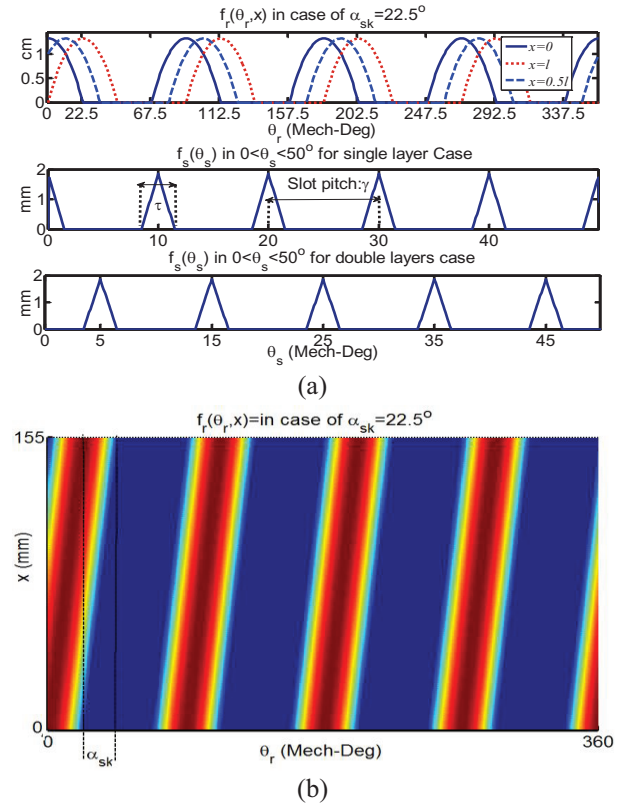
Fig. 4. Illustration of air-gap functions considering $\alpha_{sk} = 22.5°$: (a) 2-D scheme of rotor saliency and slot opening, and (b) 3-D scheme of rotor poles saliency.

IV. WINDING FUNCTION

Sinusoidal winding function is an ideal feature of the machine that is not sufficient for exact modeling purposes. In fact, limited number of slots is one of the real factors that cause winding and MMF functions to be non-sinusoidal. It should be noted that a 4-pole machine with 36 slots and 90 turns per pole is equivalent to a machine with 30 turns per slot in single-layer and 15 turns per slot in double-layer winding. Now, the winding function for phase 'A' ($N_A(\theta_s)$), is shown in Fig. 5 (a), which is obtained by considering Fig. 6 (b). Clearly, the winding function for phases 'B' and 'C' are obtained similar to phase 'A' with 120 and 240 degrees phase shift, respectively. The winding function shown in Fig. 5 (a) will be used for modeling in next sections [1]-[5] and [17].

V. INDUCTANCE COMPUTATION BY WFA

Considering $\theta_r = \theta_s - \theta_m$, winding function approach is used to calculate the machine's inductances as written in (10) (the winding functions used for calculations are shown in Fig. 5 (a)):

$$L_{ij}(\theta_m) =$$
$$\mu_0 r \int_0^l \int_0^{2\pi} N_i(\theta_s)N_j(\theta_s)f_g^{-1}(\theta_s,\theta_m,x).d\theta_s.dx. \quad (10)$$

Using the above equation for different θ_m values ($0 \leq \theta_m \leq \pi$), the inductance matrix is calculated as:

$$L(\theta_m) =$$
$$\begin{bmatrix} L_{AA}(\theta_m) + l_{ls} & L_{AB}(\theta_m) & L_{AC}(\theta_m) \\ L_{AB}(\theta_m) & L_{BB}(\theta_m) + l_{ls} & L_{BC}(\theta_m) \\ L_{AC}(\theta_m) & L_{BC}(\theta_m) & L_{CC}(\theta_m) + l_{ls} \end{bmatrix}. \quad (11)$$

In (10), $f_g(\theta_s,\theta_s,x)$ is the air-gap function which consists of three parts including rotor poles (f_r), slot opening (f_s) and conventional air-gap (g_0), as written in (9). The instantaneous machine torque is calculated as follows:

$$\tau_e(\theta_m) = \frac{1}{2} i^T \frac{dL}{d\theta_m} i. \quad (12)$$

In which, L is the machine's inductance matrix as written in (11), superscript T denotes the transpose of the matrix and i is the currents vector of stator's windings which is given as follows:

$$i(\theta_m) = [i_A(\theta_m) \quad i_B(\theta_m) \quad i_C(\theta_m)]^T. \quad (13)$$

It is important to note that a proper procedure should be employed for modeling and computing of the machine's variables such as currents, fluxes, etc., when a three-phase power is applied. Using current source as input of the machine does not model the real behavior of the latter. So, the machine's performance will be different in comparison with the real performance. Thus, a proper dynamic model for machine to calculate the currents and torque is necessary.
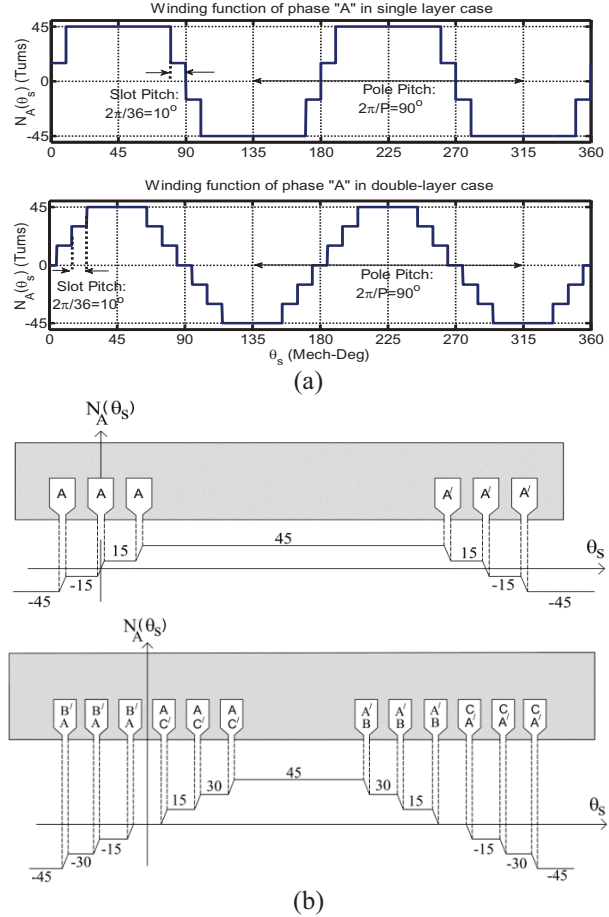
Fig. 5. (a) Winding function of phase 'A' in single and double-layer winding, and (b) slot-winding configurations.

VI. DISCRETE MODEL OF SynRM

To investigate the performance of the SynRM in steady state, we use the dynamic model of the machine. Neglecting the core losses, the motor's equations can be written as:

$$v(t) = R.i(t) + d\lambda(t)/dt, \quad (14)$$
$$\lambda(t) = L(t).i(t), \quad (15)$$
$$d\lambda(t)/dt = 1/\Delta t \, (L(t)i(t) - L(t-\Delta t)i(t-\Delta t)), \quad (16)$$
$$i(t) = (1/\Delta t.L(t) + R)^{-1}.[v(t) + 1/\Delta t.L(t-\Delta t)I(t-\Delta t)], \quad (17)$$
$$t = \theta_m/\omega_m \rightarrow \theta_m = \omega_m t \rightarrow x(\theta_m) = x(\omega_m t) \, for \, given \, x, \quad (18)$$
$$dL_{xy}(\theta_m)/d\theta_m = (L_{xy}(\theta_m + \Delta\theta_m) - L_{xy}(\theta_m))/\Delta\theta_m, \quad (19)$$
$$\Delta\theta_m = \omega_m \Delta t. \quad (20)$$

As Δt being step time, equations (16) and (19) can be used for derivation. Considering (14)-(16), the 3-

phase currents is computed by (17). Equations (19) and (20) can be used for torque computation in (12). It should be mentioned that the accuracy of the model depends on the value of Δt. In (14), R is the stator resistance matrix which is defined as:

$$R = diag[R_s].\qquad(21)$$

In which, R_s is the stator winding resistance. Also, in equations (14)-(17), $\lambda(t)$ and $v(t)$ are the stator flux and voltage vectors which are defined as:

$$\lambda = [\lambda_A \quad \lambda_B \quad \lambda_C]^T , v = [v_A \quad v_B \quad v_C]^T.\qquad(22)$$

VII. RESULTED AND DISCUSSION

In this section, the torque ripple is calculated in various scenarios. At first, as in [1], a three-phase sinusoidal current source is applied to the motor with single-layer winding in skewed and un-skewed cases and the torque ripple is calculated. Then, for the same motor with single-layer winding, in both skewed and un-skewed cases, a three-phase sinusoidal voltage is applied. The results are compared with those in [1]. It is shown that different results are obtained in voltage-source case in comparison with the current-source case. Finally, the same calculations are done for the motor with double-layer winding.

Phase 'A' self-inductance and mutual inductance between phases 'A' and 'B' of the machine in both skewed and un-skewed cases for single and double-layer winding are shown in Fig. 6. There are two kinds of harmonic components in inductances due to slot openings and distributed winding which have high and low order components, respectively. It is seen in Fig. 6 that the high frequency components have been eliminated due to pole skewing. Moreover, the low frequency components are reduced in case of double-layer winding. In fact, the slot opening effects have been eliminated due to pole skewing which can reduce the produced torque ripple.
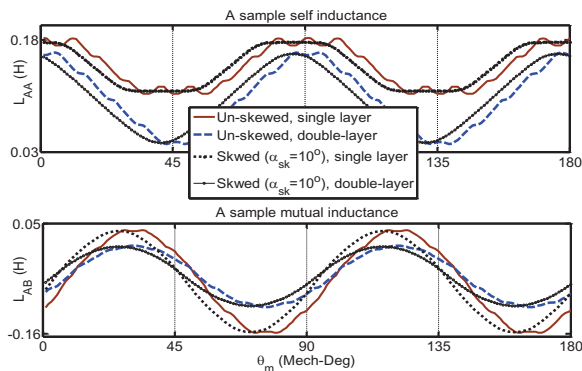
Fig. 6. The machine's inductances in single and double-layer winding, in skewed and un-skewed cases.

A. SynRM with single-layer windings

The machine with single-layer winding in skewed and un-skewed cases is simulated in this sub-section. The skewing angle is chosen $\alpha_{sk} = 10°$ in skewed case and a 50 Hz three-phase 2A current source is applied to the motor:

$$i_A(t) = 2\sqrt{2}\sin(2\pi f_s t - \varphi),$$
$$i_B(t) = 2\sqrt{2}\sin(2\pi f_s t - \frac{2\pi}{3} - \varphi),\qquad(23)$$
$$i_C(t) = 2\sqrt{2}\sin(2\pi f_s t + \frac{2\pi}{3} - \varphi).$$

The rotating speed is considered equal to synchronous speed which is 1500 RPM in 50 Hz power supply frequency. Moreover, the φ value is considered $45°$ to obtain the maximum average torque during simulation which is equal to 2.7 N.m. The output torque is calculated in both skewed and un-skewed cases. The results are illustrated in Fig. 7. It is seen that the torque has less ripple due to pole skewing. These calculations have been also carried out in [1] and [2] and the same results have been exactly obtained. Similar calculations have been done by applying the following three-phase voltages as input of the machine:

$$v_A(t) = 95\sqrt{2}\cos(2\pi f_s t - \varphi),$$
$$v_B(t) = 95\sqrt{2}\cos(2\pi f_s t - 2\pi/3 - \varphi),\qquad(24)$$
$$v_C(t) = 95\sqrt{2}\cos(2\pi f_s t + 2\pi/3 - \varphi).$$

The machine torque in both skewed and un-skewed cases are illustrated in Fig. 8. It should be mentioned that the value of the voltage source is considered 95 V to obtain the average torque of 2.7 N.m. with tuned φ value. This causes the machine's performance to be similar to that with 2A current source power supply.

As it is seen in Fig. 8, the pole skewing has not considerable effect on the torque ripple in voltage source case. The current waveform is also shown in Fig. 8. It is clear that the current has some significant harmonic components because of non-sinusoidal winding function in single-layer case. In fact, the reason for this phenomenon is the limited slot numbers for winding distribution.
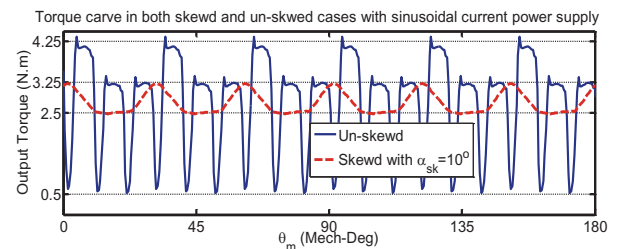
Fig. 7. Output torque in skewed and un-skewed cases with sinusoidal current source (single-layer winding).
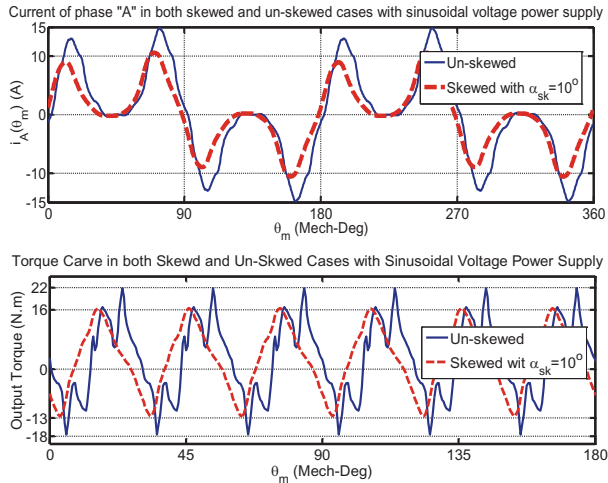
Fig. 8. Output torque and current waveform in skewed and un-skewed cases with sinusoidal voltage source (single-layer winding).

B. SynRM with double-layer winding

In this sub-section, the torque calculation for double-layer winding is performed. Figure 9 shows the output torque of machine with current source input.

In this case, a significant reduction is seen in the torque ripple. Exactly, the same results have been also reported in [1]. Comparing to Fig. 7, which has been obtained for single-layer winding, less torque ripple is produced in case of double-layer winding. Since, in reality, the voltage source power is usually supplied to the motor, (24) is considered as an input. The output torque and stator currents have been obtained for this case which is shown in Fig. 10. As it is seen in this figure, significant reduction in torque ripple is obtained in case of pole-skewed double-layer winding. This result has not been obtained in single-layer winding with voltage source power supply. As shown in Fig. 10, the machine's current has much less harmonic components than single-layer winding (see Fig. 8). In fact, the pole skewing is an effective tool for torque ripple reduction, only in cases that the machine currents have low harmonic components due to more slot numbers for each pole. In order to make better comparison, more results in different cases have been obtained which are listed in Table 2. As it is seen in the table, in current source case, the pole skewing has significant effect on the torque in both single and double-layer winding machine (about 80% reduction is seen in torque ripple); however, there is only 27.5% reduction in the torque ripple in voltage-fed single-layer winding machine. Also, in voltage-fed double-layer winding machine, the pole skewing reduces the torque ripple 84%.

Considering the results of Table 2, the effect of pole skewing on the torque ripple reduction can be summarized as follows:

✓ For sinusoidal current source-fed SynRM, the pole skewing significantly reduces the torque ripple in both single and double-layer winding cases. The ripple reductions in single and double-layer winding are 80.5% and 79%, respectively.

✓ For sinusoidal voltage source-fed SynRM, the pole arc skewing has not significant effect on the torque ripple reduction in single-layer winding case. This fact is due to generated harmonic components in the machine currents which are because of the produced space harmonics by the non-sinusoidal winding function. In this case, only 27.5% reduction is seen in the torque ripple.

✓ As an important result, the pole skewing improves the torque ripple just for the machines with sinusoidal winding function which can be obtained by multi-layer winding or more stator slot numbering.

✓ As another result, since in reality, the machine is supplied by voltage source, the pole arc skewing is an effective method for the SynRMs with the winding function having low harmonic components.
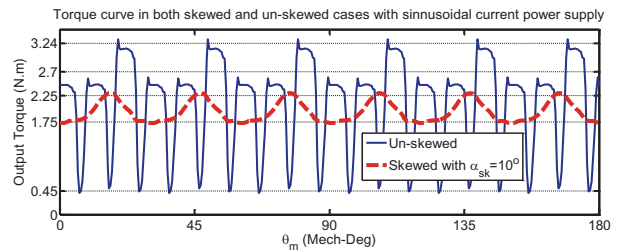
Fig. 9. Output torque in skewed and un-skewed cases with sinusoidal current source (double-layer winding).
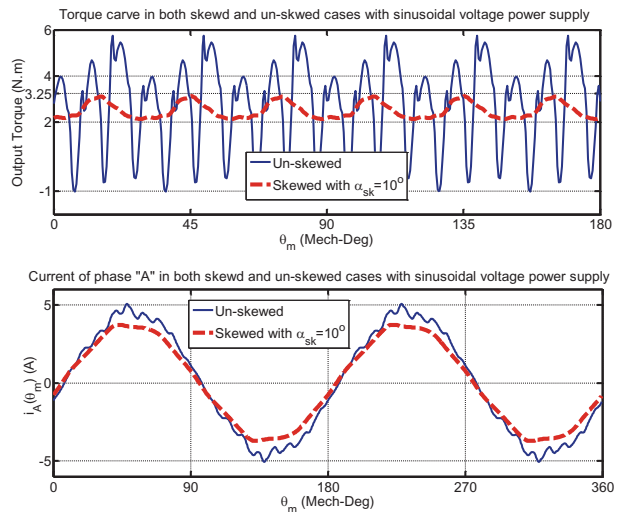
Fig. 10. Output torque and stator current in skewed and un-skewed cases with sinusoidal voltage source (double-layer winding).

Table 2: Torque ripple improvement due to pole skewing and double layer winding

	Current Source				Voltage Source			
Winding Layers	1	1	2	2	1	1	2	2
Average Torque (N.m)	2.8	2.8	2.1	2.1	2.8	2.8	2.5	2.5
Torque Ripple (%)	139	27.1	138	29.2	1428	1035	247	39.8
α_{sk}	$0°$	$10°$	$0°$	$10°$	$0°$	$10°$	$0°$	$10°$
Torque Ripple Reduction (%)	80.5		79		27.5		84	

VIII. VALIDATION OF THE RESULTS

As it is known, to analyze electrical machines, the finite element method (FEM) is an established method among researcher [1]-[4], [18]-[20]. In this section, a 3-D FEM is employed to evaluate the precision of the proposed method. The single-layer winding SynRM with un-skewed and 10° skewed poles is simulated in ANSOFT/Maxwell environment. φ value has been tuned to obtain average torque of 0 N.m for no-load condition in both FEM and proposed modeling method. It should be mentioned that the rotational speed has been considered as synchronous speed (1500 RPM) in simulations. The machine structure in Maxwell environment is shown in Fig. 11. The calculation of voltage-fed non-skewed SynRM torque in no-load condition has been done by the proposed method and compared with the results of the FEM. The results are presented in Fig. 12. The same calculations have been done for 10° skewed poles SynRM. The results are illustrated in Fig. 13. It is seen in these figures that the results obtained by the analytical calculations are close enough to the results of the FEM, validating the proposed method.
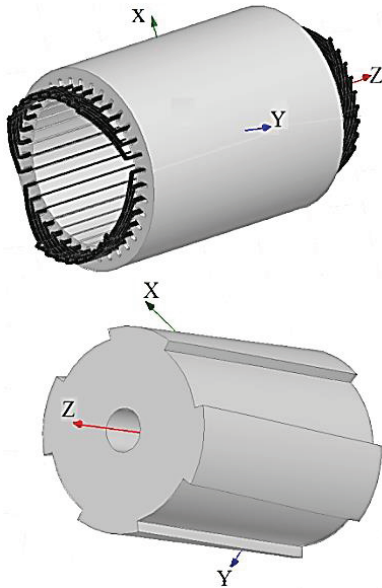
Fig. 11. Machine model in Maxwell environment.
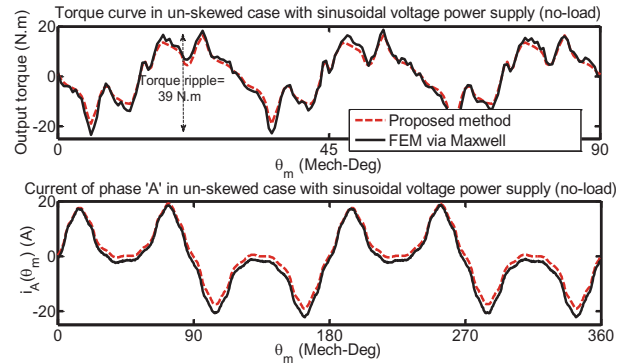
Fig. 12. Comparison of the proposed method with 3-D FEM for no-load voltage-fed machine in un-skewed case.
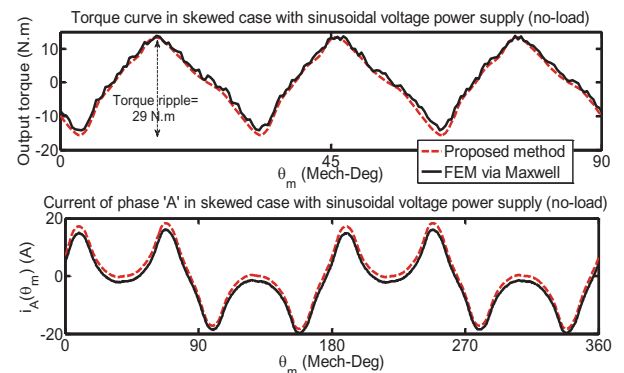
Fig. 13. Comparison of the proposed method with 3-D FEM for no-load voltage-fed machine in skewed case.

IX. CONCLUSION

In this paper, a numerical discrete-time method has been introduced to model SynRM in voltage-fed condition. An exact analytical method is proposed to calculate the currents and the torque of the motor. The proposed method has a simple procedure and can be applied to all other machines. According to the obtained results, it was shown that the pole skewing of SynRM has significant effect on the torque ripple reduction in double-layer winding machine which has lower harmonic components compared to single-layer winding. So, it is shown that the pole skewing is an

effective tool just in case that the winding function has low harmonic components which lead to semi-sinusoidal current. This case can be obtained by multi-layer windings or more slot numbers per pole. The machine has been simulated by 3-D FEM and the obtained results validate the accuracy of the proposed method.

REFERENCES

[1] T. Hamiti, T. Lubin, and A. Rezzoug, "A simple and efficient tool for design analysis of synchronous reluctance motor," *IEEE Trans. Magnetics*, vol. 44-12, pp. 4648-4652, 2008.

[2] T. Lubin, T. Hamiti, H. Razik, and A. Rezzoug, "Comparison between finite-element analysis and winding function theory for inductances and torque calculation of a synchronous reluctance machine," *IEEE Trans. Magnetics*, vol. 43-8, pp. 3406-3410, 2007.

[3] M. Jocsimovic, D. J. Penman, and N. Arthur, "Dynamic simulation of dynamic eccentricity in induction machine-winding function theory," *IEEE Trans. Energy Conversion*, vol. 15-2, pp. 143-148, 2000.

[4] J. Faiz and I. Tabatabaee, "Extension of winding function theory for non-uniform air gap in electrical machinery," *IEEE Trans. Magnetics*, vol. 38-6, pp. 3654-3657, 2002.

[5] I. Tabatabaee, J. Faiz, H. Lessani, and T. N. Razavi, "Modeling and simulation of a salient-pole synchronous generator with dynamic eccentricity using modified winding function theory," *IEEE Trans. Magnetics*, vol. 40-3, pp. 1550-1555, 2004.

[6] P. Ponomarev, P. Lindh, and J. Pyrhonen, "Effect of slot-poles combination on the leakage inductance and the performance of tooth-coil permanent-magnet synchronous machines," *IEEE Trans. Ind. Electronics*, vol. 60-10, pp. 4310-4317, 2013.

[7] T. C. Ilamparithi and S. Nandi, "Detection of eccentricity faults in three phase reluctance synchronous motor," *IEEE Trans. Ind. Applications*, vol. 48-4, pp. 1307-1377, 2012.

[8] T. Matsuo and T. A. Lipo, "Rotor design optimization of synchronous reluctance machine," *IEEE Trans. Energy Conversion*, vol. 9-2, pp. 359-365, 1994.

[9] H. Kiriyama, S. Kawano, Y. Honda, T. Higaki, S. Morimoto, and Y. Takeda, "High performance synchronous reluctance motor with multi-flux barrier for the appliance industry," in *Proc. IEEE Ind. Appl. Conf.*, vol. 1, pp. 111-117, Oct. 1998.

[10] Y. Inoue, S. Morimoto, and M. Sanada, "A novel control scheme for maximum power operation of synchronous reluctance motors including maximum torque per flux control," *IEEE Trans. Ind. Applications*, vol. 47-1, pp. 115-121, Jan./Feb. 2011.

[11] H. W. de Kock, A. J. Rix, and M. J. Kamper, "Optimal torque control of synchronous machines based on finite element analysis," *IEEE Trans. Ind. Electronics*, vol. 57-1, pp. 413-419, 2010.

[12] T. Ilamparithi and S. Nandi, "Comparison of results for eccentric cage induction motor using finite element method and modified winding function approach," *Joint Int. Conf. Power Electron., Drives, Energy Syst.*, pp. 1-7, Dec. 2010.

[13] C. Bruzzese, E. Santini, V. Benucci, and A. Millerani, "Model based eccentricity diagnosis for a ship brushless-generator exploiting the machine voltage signature analysis (MVSA)," *IEEE Int. Symp. Diag. Elect. Mach., Power Electron., Drives*, pp. 1-7, Aug./Sep. 2009.

[14] C. Bruzzese and G. Joksimovic, "Harmonic signatures of static eccentricities in the stator voltages and in the rotor current of no-load salient pole synchronous generators," *IEEE Trans. Ind. Electronics*, vol. 58-5, pp. 1606-1624, 2011.

[15] T. Ilamparithi and S. Nandi, "Analysis, modeling and simulation of static eccentric reluctance synchronous motor," *IEEE Int. Symp. Diag. Elect. Mach., Power Electron., Drives*, pp. 45-50, Sept. 2011.

[16] P. Neti and S. Nandi, "An improved strategy to detect stator inter-turn faults in synchronous reluctance motors using both negative sequence quantities and stored magnetic energy after supply disconnection," *IEEE IAS Annu. Meeting*, pp. 2234-2241, Sept. 2007.

[17] S. Saied, K. Abbaszadeh, and A. Tenconi, "Improvement to winding function theory for PM machine analysis," *Int. Conf. Power Eng., Energy and Electrical Drives*, pp. 1-6, May 2011.

[18] A. Shiri and A. Shoulaie, "Investigation of frequency effects on the performance of single-sided linear induction motor," *The Applied Computational Electromagnetics Society*, vol. 27, no. 6, 2012.

[19] E. Afjei and H. Torkaman, "Finite element analysis of switched reluctance generator under fault condition oriented towards diagnosis of eccentricity fault," *The Applied Computational Electromagnetics Society*, vol. 26, no. 1, 2011.

[20] E. Afjei, M. R. Tavakoli, and H. Torkaman, "Eccentricity compensation in switched reluctance machines via controlling winding turns/stator current: theory, modeling, and electromagnetic analysis," *The Applied Computational Electromagnetics Society*, vol. 28, no. 2, 2013.

Peyman Naderi was born in Ahvaz, Iran, in 1975. He received the B.S. degree in Electronic Engineering in 1998 and the M.S. degree in Power Engineering from Chamran University, Ahvaz, Iran in 2001. He has a Ph.D. degree in Power Engineering from K.N. Toosi University, Tehran, Iran. He is currently an Assistant Professor in Shahid Rajaee Teacher Training University of Tehran, Iran.

His interests are hybrid and electric vehicles, vehicles dynamic, power system transients and power system dynamics.

Abbas Shiri was born in Hashtrood, Iran in 1980. He received the B.Sc. degree from Tabriz University and the M.Sc. and Ph.D. degrees from Iran University of Science and Technology (IUST) in Electrical Engineering in 2004, 2006 and 2013, respectively. He is currently an Assistant Professor at Shahid Rajaee Teacher Training University, Tehran, Iran.

His areas of research interests include linear electric machines, electromagnetic systems and actuators, electrical machine design and modeling.